



ISTITUTO NAZIONALE DI RICERCA METROLOGICA Repository Istituzionale

Cerium doped zirconium dioxide as a potential new photocatalytic material. the role of the preparation method on the properties of the material

This is the author's submitted version of the contribution published as:

Original

Cerium doped zirconium dioxide as a potential new photocatalytic material. the role of the preparation method on the properties of the material / Gionco, C.; Paganini, M. C.; Chiesa, M.; Maurelli, S.; Livraghi, S.; Giamello, E.. - In: APPLIED CATALYSIS A: GENERAL. - ISSN 0926-860X. - 504:(2015), pp. 338-343. [10.1016/j.apcata.2015.02.021]

Availability:

This version is available at: 11696/66302 since: 2021-02-01T15:24:44Z

Publisher:

ELSEVIER SCIENCE BV

Published

DOI:10.1016/j.apcata.2015.02.021

Terms of use:

This article is made available under terms and conditions as specified in the corresponding bibliographic description in the repository

Publisher copyright

(Article begins on next page)

Cerium doped Zirconium dioxide as a potential new photocatalytic material. The role of the preparation method on the properties of the material.

*Chiara Gionco, Maria C. Paganini, Mario Chiesa, Sara Maurelli, Stefano Livraghi, Elio Giamello**

¹ Dipartimento di Chimica, Università di Torino and NIS, Nanostructured Interfaces and Surfaces,
Via P. Giuria 7, 10125 Torino, Italy

AUTHOR INFORMATION

Corresponding Author* elio.giamello@unito.it.

Abstract

Small amounts of Ce⁴⁺ ions dispersed in the bulk of ZrO₂ give to this material unexpected properties of photoactivity under visible light. Three different samples have been synthesized following different methods and using different precursors and all show some degree of photoactivity. This has been monitored via EPR spectroscopy in terms of charge separation (electrons and holes formation) under polychromatic light having $\lambda > 420\text{nm}$. This behavior, unimaginable for bare zirconia due to the large band gap of this oxide (around 5eV), is possible because of the presence in the solid of empty 4f Ce states located in the middle of the band gap which act as intermediate levels in a double excitation mechanism. The doped oxide here described can be considered an example of third generation photoactive material operating in visible light.

KEYWORDS: Photocatalysis, Charge Separation, EPR Spectroscopy.

Introduction

There is today a growing awareness that a major challenge facing the human kind is developing new and renewable energy sources capable of overcome the present strong dependence on fossil

fuels which is generating severe concerns for the state of the planet.[1, 2] A new ideal source should be inexpensive, abundant and clean. These criteria are met by sunlight since the sun irradiates the earth surface with a power of about 120 000 TW, much more (4 orders of magnitude) than the current energy use on our planet.[3]

It is not surprising therefore that a big effort has been done to orient the scientific research towards the exploitation of the solar light in various ways. This has occurred also within the catalytic community which is currently more and more oriented towards studies directed to exploit light energy in various kind of applications.[4] Among photochemical applications in catalysis, one has to mention quite mature approaches like photocatalytic reactions for pollutant abatement [5] and more ambitious applications aimed to synthesize solar fuels in processes inspired to the natural photosynthesis. Solar fuels, such as hydrogen (from water photosplitting) or methanol and other chemicals (from carbon dioxide reduction) have to be regarded as true chemical energy storage system which will be hopefully prepared in suitable solar factories by means of efficient processes of sunlight harvesting. While several practical applications of environmental photocatalysis are nowadays available (indoor air purification [6, 7], water decontamination [8]) the large scale commercial production of solar fuels is however still a dream due to the difficulty in finding suitable artificial systems having high efficiency, long term stability and low cost.

The basic component of a photocatalytic system is a semiconductor capable of generating a phenomenon of charge separation by absorbing light. The electron (excited in the conduction band) and the hole (consequently formed in the valence band) are potentially the agents of a reduction and of an oxidation reaction respectively.[9] Due to the intrinsic difficulty of these reactions the whole system is in some cases integrated by a reduction and an oxidation co-catalyst. To achieve high performances of the whole photocatalytic system it is necessary to develop semiconductors having excellent electronic properties and, in parallel, co-catalysts having high efficiency.

Among the semiconductors employed in photocatalytic reactions, transition metal oxides play a paramount role due to their qualities in term of stability in various media often accompanied by low or reasonable cost. The search for innovative materials in these field is oriented to select systems having a suitable electronic structure capable of harvesting solar light at the earth surface (which means essentially visible light) and excellent potential to perform the desired redox process. This is practically impossible to be found in a unique system. Large band gap values

correspond to good reduction and oxidative potentials but inevitably also need absorbing high energy photons (UV light, scarcely present in solar irradiation at the earth surface) to perform the charge separation. On the other hand a semiconductor with smaller band gap value, compatible with visible light absorption, cannot have satisfactory potentials for both reduction and oxidation. To overcome this limitation many approaches have been developed for example by coupling two different semiconductors in a so called Z-scheme, (each semiconductor deals with one of the two semi-reaction) a scheme directly inspired to natural photosynthesis.[4]

An alternative possibility is to modify a semiconductor with relatively large band gap in order to make possible the absorption of visible light. This has been intensely done in the case of titanium dioxide, the most used and investigated solid in the field of photocatalysis, following more than an approach (doping with transition metal ions [10], anchoring small metal particles exhibiting plasmonic effects [11], doping with non metal atoms[12-14]) and with contradictory results. In the present paper we intend to analyze the modification of the light absorption mechanism induced by engineering the band gap of ZrO_2 using tiny concentrations of cerium ions. In particular we want to show how, using low energy photons and in spite of the relatively large band gap value of the oxide, it is possible to perform charge separation conveying electrons in the conduction band and generating holes in the valence band. The general purpose of the present paper is to indicate a methodology which can potentially lead, after a severe screening of many systems, to find a new set of materials on which concentrate efforts and further studies. The final aim of this research is the identification of novel photoactive materials for advanced photocatalytic applications.

Experimental

Preparation of the samples

In the present investigation three Ce doped ZrO_2 materials have been synthesized using distinct preparation methods. All materials have the same composition corresponding to a CeO_2 molar fraction of 0.005 (0.5%). All reactants employed in this work were purchased from Aldrich except for Ce isopropoxide that was purchased from Alfa Aesar. All reactants were used without any further purification treatment. All the reactants have purity higher than 99.9% and do not contain traces of lanthanides.

Two of the three samples of mixed Ce-Zr oxides were prepared via sol-gel synthesis. The first sol gel sample was prepared mixing a first solution (0.45M, solution A) made dissolving Ce

isopropoxide in 2-propanol and tetrahydrofuran (2-propanol:THF ratio 5:1) with a second solution (0.2 M, solution B) made dissolving Acetylacetone in 2-propanol. Finally a third solution (solution C) was prepared dissolving water in 2-propanol. Solution B was then added to Solution A obtaining solution D. The stoichiometric amount of solution D was then added to 7ml of Zr propoxide and finally 5ml of solution C were added in order to start hydrolysis. This sample will be hereafter labelled as CZ05_SGI where SG stands for sol-gel and I for isopropoxide.

The second sample synthesized via sol gel process was prepared mixing a solution of $\text{Ce}(\text{NO}_3)_3 \cdot 6\text{H}_2\text{O}$ in water with a solution of Zr propoxide in propanol. The volume ratio Alcoxide:Alcool:Water was 2:2:1. This sample will be hereafter labelled as CZ05_SGN where N is for Nitrate. Both the sols produced by hydrolysis has been aged in air until the formation of a gel which was then dried at 333K. Finally the powder was calcined at 773 K in air for 2 hours.

The third sample has been prepared via an hydrothermal process starting from a 1.0 M aqueous solution containing the stoichiometric ratio of $\text{ZrOCl}_2 \cdot 8\text{H}_2\text{O}$ and $\text{Ce}(\text{SO}_4)_2$. The pH was then adjusted to 11 using a 4.0 M NaOH aqueous solution, inducing the formation of a gel. The gel was then transferred into a 100ml Teflon-lined stainless steel autoclave, which was heated in oven at 200°C overnight. This third sample will be indicated as CZ05_HYD.

Characterization techniques

Powder X-rays diffraction (XRD) patterns were recorded with a PANalytical PW3040/60 X'Pert PRO MPD using a copper K_α radiation source (0.15418 nm). The intensities were obtained in the 2θ ranges between 20° and 80°. The X'Pert High-Score software was used for data handling. The MAUD 2.26 software was used for Rietveld refinement. To determine the instrumental function the pattern obtained by a well crystallized silicon standard (crystallite size = 1 μm) was used. The UV-Vis absorption spectra were recorded using a Varian Cary 5000 spectrometer, coupled with an integration sphere for diffuse reflectance studies, using a Carywin-UV/scan software. A sample of PTFE with 100% reflectance was used as reference.

Electron Paramagnetic Resonance (EPR) spectra, recorded at liquid nitrogen temperature, were run on a X-band CW-EPR Bruker EMX spectrometer equipped with a cylindrical cavity operating at 100 kHz field modulation. The effect of light on EPR spectra was investigated irradiating the sample in the EPR resonant cavity by a 1000 W mercury/Xenon lamp (Oriel Instruments) equipped with a IR water filter to avoid over-heating and using a cut-off at 420nm to exclude UV radiation. The spectra were recorded in situ during the irradiation.

Results

X-Ray powder diffraction analysis

Figure 1 shows the XRD patterns obtained for the three samples (CZ05_SGI, CZ05_SGN and CZ05_HYD). The XRD patterns show that there is no evidence of any reflection peak typical of the CeO₂ fluoritic phase; only zirconia phases are present. While in *Table 1* all parameters used in the Rietveld refinement done using the MAUD software are reported.

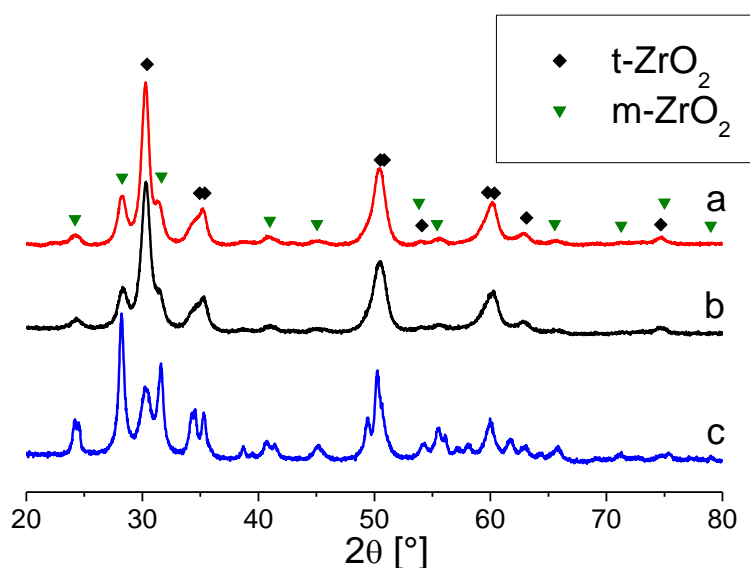


Figure 1 XRD patterns of (a) CZ05_SGI (b) CZ05_SGN, (c) CZ05_HYD

For all samples two phases can be identified from XRD analysis, tetragonal and monoclinic zirconia respectively. In particular for the two samples prepared via sol-gel (Figure 1.a and 1.b) a clear predominance of the tetragonal phase can be observed, whereas the sample CZ05_HYD shows the predominant presence of the monoclinic phase of zirconia (around 70% see *Table 1*). The XRD peaks are broad, indicating the formation of small crystallites, as evidenced in *Table 1*.

It is well-known that the fraction of m-ZrO₂ tends to decrease with increasing the dopants content [15] indicating the preferential stabilization of tetragonal zirconia in the presence of Ce ions into the structure. In the present case, however, the Ce percentage in the various samples is constant, so that the different phase composition between samples prepared via sol-gel and that prepared via hydrothermal synthesis is amenable to the synthetic route used.

Table 1. Weight percentage (%wt), lattice parameters (a, b, c, β) and crystallite dimension (d) obtained from Rietveld refinement of the XRD patterns of bare and mixed Ce-Zr oxides. R_{wp} is the weighted residual error.

Sample	R_{wp} [%]	Phase	%wt	a [Å]	b[Å]	c[Å]	β [°]	d [nm]
CZ05_SGI	1.45	t-ZrO ₂	57	3.60	3.60	5.18	/	16
		m-ZrO ₂	43	5.15	5.20	5.33	99.00	12
CZ05_SGN	4.85	t-ZrO ₂	64	3.60	3.60	5.17	/	14
		m-ZrO ₂	36	5.14	5.19	5.32	98.88	15
CZ05_HYD	5.47	t-ZrO ₂	32	3.60	3.60	5.16	/	10
		m-ZrO ₂	68	5.16	5.20	5.32	99.5	24

Diffuse Reflectance UV-Vis spectroscopy.

UV-Vis spectra obtained by diffuse reflectance spectroscopy are reported in figure 2 where the optical behavior of the mixed materials are compared with that of the bare zirconium dioxide. The classic band gap transition of bare zirconia (an insulator) falls, as expected, at about 250 nm (5.08eV). The UV spectrum of cerium dioxide (here not reported)[16], shows an optical transition at about 460 nm (2.98eV) due to the excitation of electrons from the valence band to 4f orbital states. The difference from the top of the valence band and the bottom of the conduction band (5s and 5d states) in cerium dioxide is, according to theoretical calculations, about 6eV.[17, 18] All the doped samples here examined, though containing a modest concentration of the dopant, show transition with a pronounced red-shift with respect to zirconia. In particular the sample obtained by hydrothermal process presents the highest red shift, immediately followed by the sol-gel prepared CZ05_SGI. In the part B of the figure where the optical activity is reported in terms of the Kubelka-Munck function, it can be better distinguished the dramatic effect of cerium doping on the optical properties of the material. A relatively modest concentration of cerium brings about a relevant red shift of the absorption for all samples. A tail of this absorption lies clearly within the visible region. This result indicates that in all samples a relevant degree of dispersion of the dopant in the matrix has been attained.

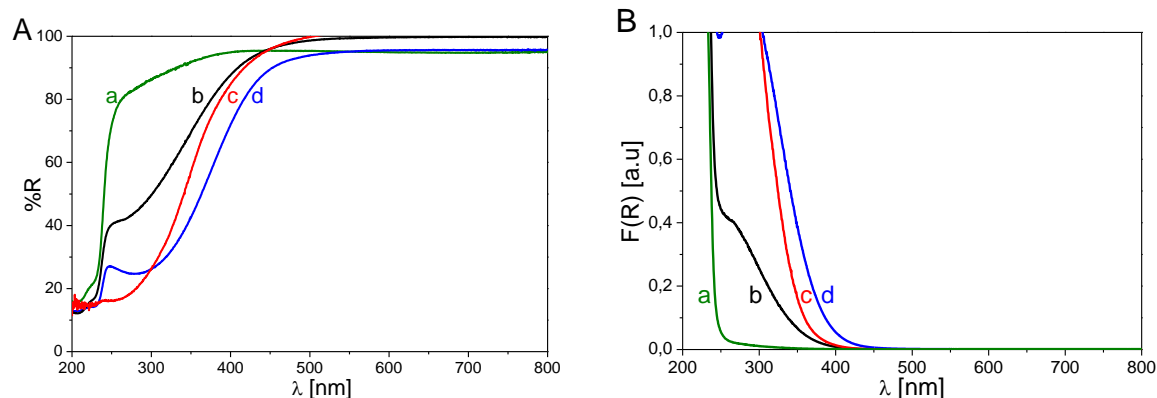
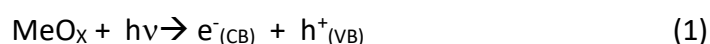


Figure 2. A) Absorption spectra of ZrO₂ (a), CZ05_SGI (b), CZ05_SGN (c) and CZ05_HYD (d). B) Absorbance spectra in the same order.

EPR spectroscopy of irradiated materials.

EPR is a suitable technique to monitor the charge separation processes. This was first shown, in the case of TiO₂, by the work of Graetzel and Howe[19-21] and by that of the Thurnauer group[22] who were able to directly monitor the spectral trace of both excited electrons and holes upon irradiation of a colloidal suspension of the oxide in water. The same experiment can be performed, though less efficiently, under vacuum as shown by some of us in the case of titania based photoactive solids [14, 23]. The direct charge separation is obtained irradiating the solid in situ at the temperature of liquid nitrogen to avoid the rapid recombination of the carriers.

In the case of a generic oxide the reaction occurring is :



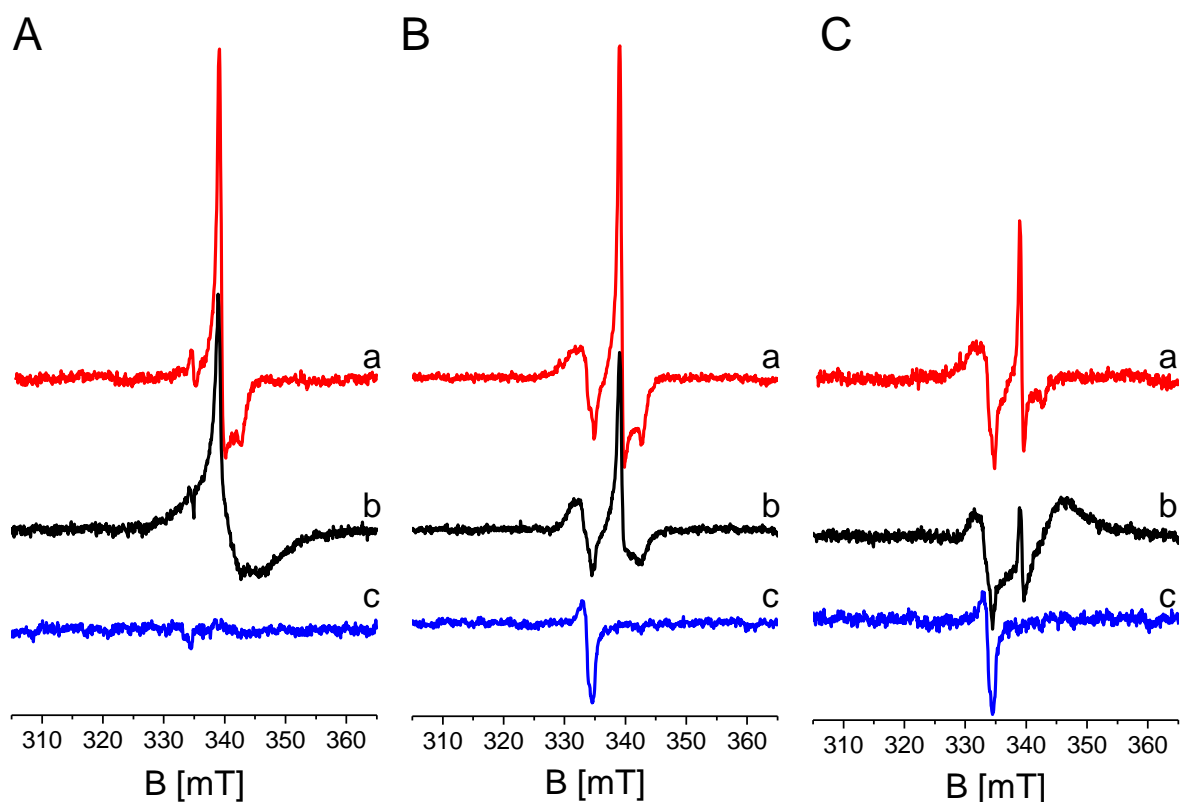


Figure 3. EPR spectra of CZ05 materials in various conditions. A: background; B: irradiation under vacuum, C) traces obtained by subtraction of the spectra in panel A from the corresponding ones in Panel B. CZ05_SGI (a), CZ05_SGN (b), CZ05_HYD (c). All spectra in panel B have been recorded under vacuum at 77K during irradiation with visible light ($\lambda > 420\text{nm}$).

If the two photogenerated charge carriers are stabilized by the solid this occurs at different sites of the oxide, usually a cation for the electron and an oxide anion for the hole. In our case formation of Zr^{3+} ($\text{Zr}^{4+} + e^- \rightarrow \text{Zr}^{3+}$) and O^- ($\text{O}^{2-} + h^+ \rightarrow \text{O}^-$) which are both paramagnetic and EPR visible is expected. Preliminary results from our group have shown some photoactivity under visible light of a Ce doped ZrO_2 material prepared via sol-gel.[16] In the present case we have followed (Fig. 3) the charge separation in the case of the three types of samples described before irradiating the solids kept under vacuum and applying a cut off to the lamp output at 420nm. The background spectra (sample in the dark) are reported in Panel A of Fig. 3. It is interesting to note that the background spectrum is not the same in the three cases. In particular the solid prepared by the hydrothermal method exhibits a flat line (Fig. 3Ac) while both sol-gel prepared materials (Fig 3Aa and 3Ab) show an EPR signal ($g_{||}=1.977$ and $g_{\perp}=1.959$). This axial signal is the same observed in the

case of bare ZrO_2 and it is due to Zr^{3+} ions always present as defects in the materials synthesized via sol gel process.[16, 24] The hydrothermal synthesis not only leads to a different phase composition with respect to the sol-gel method but also eliminates the presence of reduced, Zr^{3+} defective centers. The effect of visible irradiation ($\lambda > 420 \text{ nm}$, $h\nu < 2.95 \text{ eV}$) has a common point for the three samples that is the formation of a signal in the region at $g > 2.0$ typical of holes stabilized on oxygen ions (i.e. O^- ions).[25] At variance, the effect at higher magnetic field ($g < 2$, the spectral region typical of trapped electrons) is different in the three cases (Fig. 3, Panels B and C, where panel C report the subtraction of the spectra in A from those in B). The CZ05_SGI sample (Fig. 3, lines a) shows an increase of the of the Zr^{3+} signal upon irradiation which parallels the O^- formation. CZ05_SGN (lines b) has an opposite behaviour as the starting intensity of the Zr^{3+} signal decreases while, in the case of CZ05,_HYD (lines c) no variation in the region of Zr^{3+} centers is observed. The effect of irradiation is better evidenced in Fig. 4 which shows the trace of the trapped electrons and of the trapped holes.

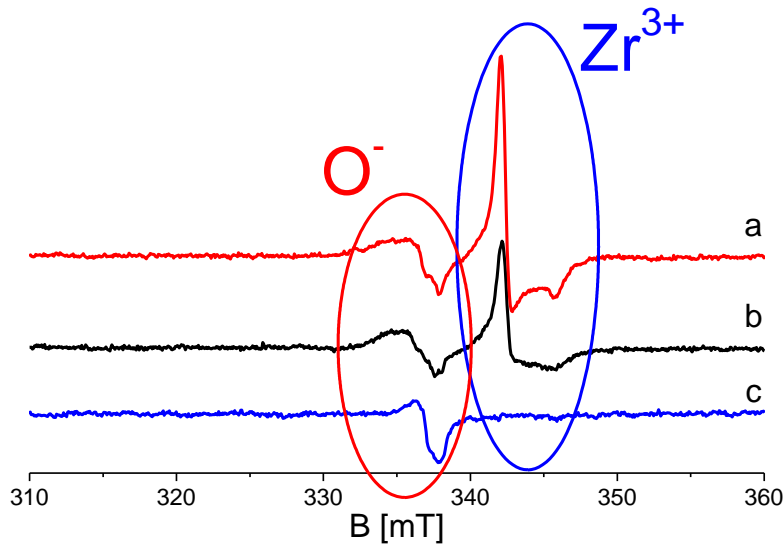


Figure 4. EPR spectra evidencing the formation of trapped charge carriers upon irradiation under vacuum ($\lambda > 420 \text{ nm}$) of a) CZ05_SGI, b) CZ05_SGN, c) CZ05_HYD.

The formation of holes in all systems caused by irradiation with wavelengths higher than 420 nm indicates that a charge separation is actually induced in the solid by photons having energy far lower than that of the ZrO_2 band gap. The different behaviour of the three samples in terms of Zr^{3+} formation is due to the fact that the as-prepared materials have not the same concentration of defects (vide infra). Photogenerated electrons are, however, produced in all cases as shown by Fig.

5 which reports the effect of irradiation of the three materials kept under oxygen atmosphere (10 mbar). In all cases in fact the trace of the EPR signal of a superoxide anion adsorbed on a Zr^{4+} surface ion is observed [24, 26] which is due to the reduction of gaseous oxygen by the photogenerated electron ($\text{e}^- + \text{O}_{2(\text{gas})} \rightarrow \text{O}_{2^-}^-(\text{ads})$).

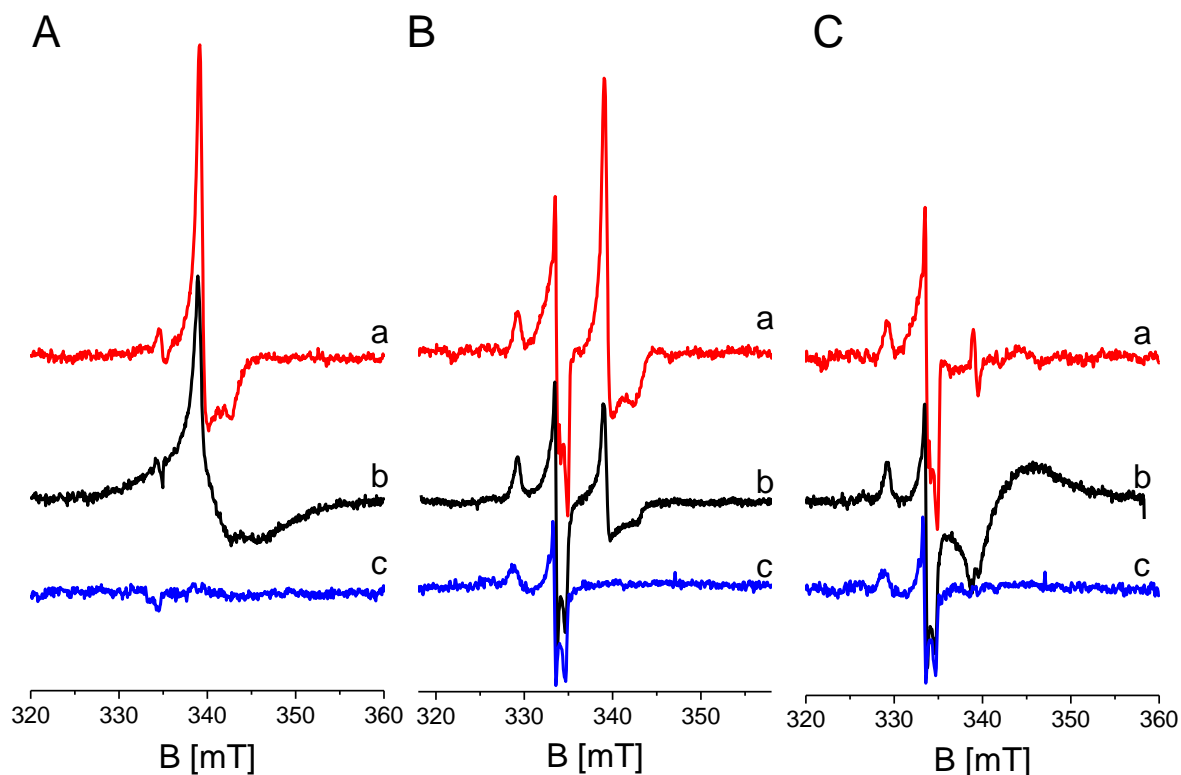


Figure 5. EPR spectra of CZ05 materials in various conditions. A: background; B: irradiation under Oxygen atmosphere, C) traces obtained by subtraction of the spectra in panel A from the corresponding ones in Panel B. CZ05_SGI (a), CZ05_SGN (b), CZ05_HYD (c). All spectra in panel B have been recorded under vacuum at 77K after irradiation with visible light ($\lambda > 420\text{nm}$) under O_2 atmosphere.

Discussion and Conclusions

The applications of zirconium dioxide in photocatalysis are very few if compared to the commonly employed titanium dioxide. However some reports are available concerning both photocatalytic oxidation of chemicals [27-30] and, with more convincing results, in the field of water photosplitting and carbon dioxide photoreduction.[31-33]

The band energy levels of ZrO_2 are in principle extremely likeable for photocatalytic applications. In particular the lowest potential of the conduction band is at about -1.0 V (vs. NHE, pH=0), i.e. much more negative than that of TiO_2 which is close to zero, and the highest potential in the valence band of ZrO_2 is around +4.0 V i.e. quite more positive than that of TiO_2 (+2.95 V). A part from comparison of the surface chemistry of the two oxides, which is certainly important in the perspective of photocatalytic phenomena but not in discussion here, the major drawback limiting the photocatalytic applications of ZrO_2 is its band gap value which is, as a consequence of the particularly favorable values of the VB and CB potentials, particularly high (5.0 eV). This value corresponds to UV frequencies, necessary to perform charge separation, practically absent in the solar radiation reaching the earth surface, thus dissuading from the search of practical applications of bare ZrO_2 using sun light.

The set of experimental data discussed in the previous sections clearly indicates that it is possible, through the dispersion of small amounts of cerium ions within the matrix of zirconium dioxide, to markedly modify the optical properties of the oxide itself. Thereby, the modified oxide becomes photoactive in visible light. This is demonstrated by the fact that a set of radiations with a wavelength higher than 420nm (i.e. with energy lower than 2.95 eV) are able to generate holes and electrons. The reason for the described photoactivity derives from the inclusion of cerium ions in the matrix which leads to the formation of intra band gap states based on the 4f levels of these ions. These empty states act as a sort of link between the valence band and the conduction band of the oxide allowing low-energy photons to excite electrons from one band to the other (Fig. 6).

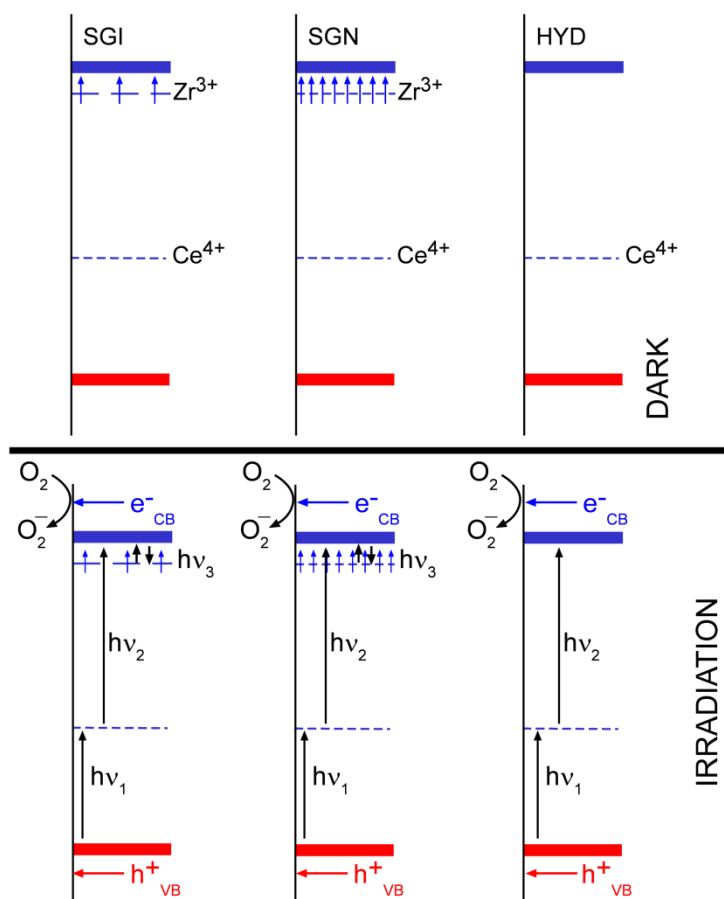


Figure 6. Schematic illustration of the electronic structure of the three materials in the dark (upper part) and under irradiation (lower part). The figure evidences the documented formation of holes, electrons and superoxide using photons with energy far lower than the band gap.

The mechanism, a sort of double jump photoexcitation, is analogous to that recently described by some of us to interpret the photocatalytic activity of N doped TiO_2 in visible light.[14] A first type of photons provides the excitation of the electrons from the valence band to the Ce intra band gap states, a second one promotes the excited electrons into the conduction band.

There is an apparent analogy between the present system and those based on the insertion of ions of the first transition series (3d) in the titanium dioxide matrix which was long experienced in the past [10, 24] to confer visible light photochemical activity to the solid. That approach was basically unsuccessful due to the onset of electron-hole recombination induced by the transition metal impurity. The analogy however is only apparent as in the present case Ce^{4+} impurities introduce empty 4f states in the system whereas in the case of transition ions in TiO_2 the recombination occurs due to the fact that 3d states, introduced at mid gap, are partially populated. This factor (empty states as mid gap levels) seems to be essential to ensure a certain efficiency to the two-photons excitation mechanism. In this work we have also shown that three

alternative preparation methods lead to distinct systems which all show, however, some photoactivity in visible light. Remarkably, in the case of CZ05_SGN and, in particular, of CZ05_HYD the precursors of the active solids are less expensive than in the case of CZ05_SGI. The different behavior of the three samples in localizing the photogenerated electrons, resumed by the results in Fig. 3, can be shortly discussed as follows. Both samples obtained via sol-gel contains Zr^{3+} ions before irradiation. These defects lie, as shown by theoretical calculations [23], in the band-gap, some tenth of eV below the limit of the conduction band. The presence of these defects in the starting materials is usually due to some effect of charge compensation. This can be either the compensation of a pentavalent impurity (e.g. Me^{5+}) or that of an oxygen vacancy (two Zr^{3+} for one oxygen vacancy). Their occurrence in sol-gel prepared samples only, indicates that with this method one obtains more defective solids than in case of the hydrothermal synthesis. The presence of occupied intra band gap states implies that their concentration can vary during the irradiation experiments since in the polychromatic light used there are infra-red components capable of exciting them in the conduction band. The interplay between electron excitation and stabilisation can explain the variability of the Zr^{3+} intensity observed for the two sol-gel samples. Despite these variation it remains that all samples are capable to generate holes and electrons. The electrons, in particular, have been monitored also in terms of surface superoxide formation which is indicative of their presence and reactivity at the surface of the solid.

To conclude, the set of data here discussed clearly indicate that it is possible, through the dispersion of small amounts of cerium ions within the matrix of zirconium dioxide, to make it photosensitive to visible light. Similar results are obtained using different precursors and different synthetic procedures for the preparation. Ce^{4+} inclusion, in fact, leads to the formation of intra band gap states based on the Ce 4f levels which act as a bridge between the valence band and the conduction band of the oxide allowing low-energy photons to excite electrons from one band to the other. The mechanism is exactly that designed by N. Serpone and coworkers while forecasting the nature of the photocatalysts of third generation.[34, 35] Ce-ZrO₂ has therefore to be considered as a member of this new family. A great deal of work is now needed to investigate the actual efficiency of the system in various photocatalytic processes and to individuate the optimal conditions (Ce loading, solid structure, crystal morphology, preparation procedures etc.) to optimize its activity and selectivity performances. Further activities must be also devoted to individuate other members of this new generation of photoactive materials for chemical

applications based on wide band gap oxides and capable to exploit visible and even NIR frequencies abundantly present in the solar spectrum.

Acknowledgment

One of the authors (EG) remembers with particular gratitude the first EPR spectra he recorded, years ago, under the careful and competent guidance of Jacques Vedrine.

Firb, cariplo, prinmedana, photomat

References

- [1] V.B. Nicola Armaroli, *Energy for a Sustainable World: From the Oil Age to a Sun-Powered Future*, Wiley-VCH Verlag GmbH & Co., London, 2011.
- [2] G.A. Olah, G.K.S. Prakash, A. Goepfert, *Journal of the American Chemical Society*. 133 (2011) 12881-12898.
- [3] J. Barber, *Chemical Society Reviews*. 38 (2009) 185-196.
- [4] K. Maeda, K. Domen, *Journal of Physical Chemistry Letters*. 1 (2010) 2655-2661.
- [5] S. S.L., *New and Future Developments in Catalysis: Solar Photocatalysis 2014*.
- [6] J. Lyu, L. Zhu, C. Burda, *Catalysis Today*. 225 (2014) 24-33.
- [7] C. Hu, Y. Cai, J. Wu, B. Yan, X. Qiu, H. He, L. Zhang, Y. Yu, in: H. Li, Q. Xu, H. Ge (Eds.), *Environmental Engineering*, Pts 1-4, 2014, pp. 1360-1363.
- [8] G.P. Anipsitakis, D.D. Dionysiou, *Applied Catalysis B-Environmental*. 54 (2004) 155-163.
- [9] A. Fujishima, X. Zhang, D.A. Tryk, *Surface Science Reports*. 63 (2008) 515-582.
- [10] M. Takeuchi, H. Yamashita, M. Matsuoka, M. Anpo, T. Hirao, N. Itoh, N. Iwamoto, *Catalysis Letters*. 67 (2000) 135-137.
- [11] S.C. Warren, E. Thimsen, *Energy & Environmental Science*. 5 (2012) 5133-5146.
- [12] R. Asahi, T. Morikawa, T. Ohwaki, K. Aoki, Y. Taga, *Science*. 293 (2001) 269-271.
- [13] S. Livraghi, M.C. Paganini, E. Giamello, A. Selloni, C. Di Valentin, G. Pacchioni, *Journal of the American Chemical Society*. 128 (2006) 15666-15671.
- [14] G. Barolo, S. Livraghi, M. Chiesa, M.C. Paganini, E. Giamello, *Journal of Physical Chemistry C*. 116 (2012) 20887-20894.
- [15] C. Gionco, A. Battiato, E. Vittone, M.C. Paganini, E. Giamello, *Journal of Solid State Chemistry*. 201 (2013) 222-228.
- [16] C. Gionco, M.C. Paganini, E. Giamello, R. Burgess, C. Di Valentin, G. Pacchioni, *Journal of Physical Chemistry Letters*. 5 (2014) 447-451.
- [17] J.L.F. Da Silva, M.V. Ganduglia-Pirovano, J. Sauer, V. Bayer, G. Kresse, *Phys. Rev. B*. 75 (2007) 035109.
- [18] D.A. Andersson, S.I. Simak, B. Johansson, I.A. Abrikosov, N.V. Skorodumova, *Phys. Rev. B*. 75 (2007).
- [19] R.F. Howe, M. Gratzel, *J. Phys. Chem.* 89 (1985) 4495-4499.
- [20] R.F. Howe, M. Gratzel, *J. Phys. Chem.* 91 (1987) 3906-3909.
- [21] R.F. Howe, M. Gratzel, *Journal of Physical Chemistry*. 91 (1987) 3906-3909.
- [22] O.I. Micic, Y.N. Zhang, K.R. Cromack, A.D. Trifunac, M.C. Thurnauer, *J. Phys. Chem.* 97 (1993) 13284-13288.
- [23] M. Chiesa, M.C. Paganini, S. Livraghi, E. Giamello, *Physical Chemistry Chemical Physics*. 15 (2013) 9435-9447.
- [24] C. Gionco, M.C. Paganini, E. Giamello, R. Burgess, C. Di Valentin, G. Pacchioni, *Chem. Mater.* 25 (2013) 2243-2253.
- [25] M. Chiesa, E. Giamello, C. Di Valentin, G. Pacchioni, *Chemical Physics Letters*. 403 (2005) 124-128.

- [26] E. Giamello, M. Volante, B. Fubini, F. Geobaldo, C. Morterra, *Materials Chemistry and Physics*. 29 (1991) 379-386.
- [27] S.G. Botta, J.A. Navio, M.C. Hidalgo, G.M. Restrepo, M.I. Litter, *J. Photochem. Photobiol. A*. 129 (1999) 89-99.
- [28] D. Fang, Z. Luo, S. Liu, T. Zeng, L. Liu, J. Xu, Z. Bai, W. Xu, *Opt. Mater.* 35 (2013) 1461-1466.
- [29] X.Z. Fu, L.A. Clark, Q. Yang, M.A. Anderson, *Environ. Sci. Technol.* 30 (1996) 647-653.
- [30] Z. Shu, X. Jiao, D. Chen, *CrystEngComm*. 14 (2012) 1122-1127.
- [31] Y. Kohno, T. Tanaka, T. Funabiki, S. Yoshida, *Chem. Commun.* (1997) 841-842.
- [32] Y. Kohno, T. Tanaka, T. Funabiki, S. Yoshida, *J. Chem. Soc. Faraday Trans.* 94 (1998) 1875-1880.
- [33] K. Sayama, H. Arakawa, *J. Phys. Chem.* 97 (1993) 531-533.
- [34] A.V. Emeline, V.N. Kuznetsov, V.K. Ryabchuk, N. Serpone, *Environmental Science and Pollution Research*. 19 (2012) 3666-3675.
- [35] N. Serpone, A.V. Emeline, *Journal of Physical Chemistry Letters*. 3 (2012) 673-677.